

GMFlow: Learning Optical Flow via Global Matching

Haofei Xu^{1*} Jing Zhang² Jianfei Cai¹ Hamid Rezatofghi¹ Dacheng Tao³

¹Department of Data Science and AI, Monash University

²The University of Sydney ³JD Explore Academy

Abstract

Learning-based optical flow estimation has been dominated with the pipeline of cost volume with convolutions for flow regression, which is inherently limited to local correlations and thus is hard to address the long-standing challenge of large displacements. To alleviate this, the state-of-the-art method, i.e., RAFT [38], gradually improves the quality of its predictions by producing a sequence of flow updates via a large number of iterative refinements, achieving remarkable performance but slowing down the inference speed. To enable both high accuracy and efficiency optical flow estimation, we completely revamp the dominating flow regression pipeline by reformulating optical flow as a global matching problem. Specifically, we propose a GMFlow framework, which consists of three main components: a customized Transformer for feature enhancement, a correlation and softmax layer for global feature matching, and a self-attention layer for flow propagation. Moreover, we further introduce a refinement step that reuses GMFlow at higher-resolutions for residual flow prediction. Our new framework outperforms 32-iteration RAFT’s performance on the challenging Sintel benchmark, while using only one refinement and running faster, offering new possibilities for efficient and accurate optical flow estimation. Code will be available at github.com/haofeixu/gmflow.

1. Introduction

Since the pioneering learning-based work, FlowNet [10], optical flow has been regressed with convolutions for a long time [15–17, 30, 35, 38, 44, 49]. To encode the matching information into the network, the cost volume (i.e., correlation) [13] was shown to be an effective component and thus has been extensively used in popular frameworks [16, 35, 38]. However, such regression approaches have a major intrinsic limitation. That is, the cost volume requires a predefined size, as the search space is viewed as the channel dimension for subsequent regression with convolutions.

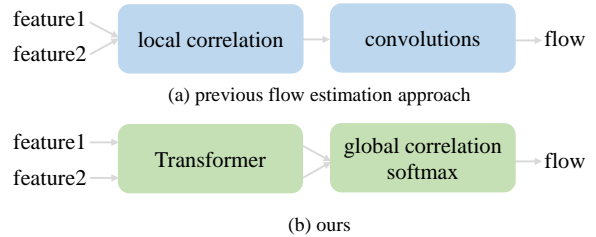


Figure 1. **Conceptual comparison of flow estimation approaches.** Most previous methods regress optical flow from a local cost volume (i.e., correlation) with convolutions, while we perform global matching with a Transformer and differentiable matching layer (i.e., correlation and softmax).

This requirement restricts the search space to a local range, making it hard to handle large displacements.

To alleviate the large displacements issue, RAFT [38] proposes an iterative framework with a large number of iterative refinements where convolutions are applied to different local cost volumes at different iteration stages so as to gradually reach near-global search space, achieving outstanding performance on standard benchmarks. The current state-of-the-art methods [17, 38, 44, 49] are all based on such an iterative architecture. Despite the excellent performance, such a large number of sequential refinements introduce linearly increased inference time, which makes it hard for speed optimization and hinders its deployment in real-world applications. This raises a question: *Is it possible to achieve both high accuracy and efficiency while without requiring such a large number of iterative refinements?*

We notice that another visual correspondence problem, i.e., sparse matching between an image pair [33, 37, 41], which usually features a large viewpoint change and is typically used for tasks like structure-from-motion, moves into a different track. The top-performing sparse methods (e.g., SuperGlue [33] and LoFTR [37]) adopt Transformers [39] to reason about the mutual relationship between feature descriptors, and the correspondences are extracted with an explicit matching layer (e.g., softmax layer).

Inspired by sparse matching, in this paper, we propose to completely remove the additional convolutional layers operating on a predefined local cost volume, and reformu-

*Work done during Haofei’s internship at JD Explore Academy

late optical flow as a *global matching* problem between two sets of deep features, which is distinct from all the previous learning-based optical flow estimation methods. Fig. 1 provides a conceptual comparison of these two flow estimation approaches. Our flow prediction is obtained with a differentiable matching layer, *i.e.*, correlation and softmax layer, by comparing feature similarities. Such a formulation calls for more discriminative feature representations, for which the Transformer [39] becomes a natural choice.

We would like to point out that although our pipeline shares the conceptual major components (*i.e.*, Transfromer and the softmax matching layer) with sparse matching [33, 37], our motivation is originated from the development of optical flow methods and the challenges associated with formulating optical flow as a global matching problem are quite different. Optical flow focuses on dense correspondences for every pixel and modern learning-based optical flow architectures are all based on a local cost volume. The scale and complexity of optical flow are much higher. Moreover, optical flow needs to deal with occluded and out-of-boundary (*i.e.*, moving out of image plane) pixels, for which simple softmax-based matching will not be effective.

Therefore, in this paper we propose a framework to realize the global matching formulation for optical flow estimation, which is named GMFlow. Specifically, the dense features extracted from a backbone network are fed into a Transformer that consists of self- and cross-attentions to obtain more discriminative refined features. We then compute the matching probability by correlating all pairwise features. After that, the flow prediction is obtained with a differentiable softmax matching layer. To address occluded and out-of-boundary pixels, GMFlow further incorporates an additional self-attention layer to propagate the high-quality flow prediction from matched regions to unmatched regions by exploiting the self-similarity in the image. Moreover, to take into account higher-resolution features for performance boosting, we further propose a refinement step, where we construct the refinement as a residual flow learning problem and resolve it by simply reapplying our GMFlow framework at each local window. Our full framework achieves competitive performance and higher efficiency compared with the state-of-the-art methods. Specifically, with only one refinement, our method outperforms 32-iteration RAFT’s performance on the challenging Sintel dataset, while running faster (see Fig. 4).

Our major contributions can be summarized as follows:

- We reformulate the prevailing optical flow learning pipeline of cost volume with convolutions into a dense global matching problem, which effectively addresses the long-standing challenge of large displacements in optical flow literature [1–3, 7, 43].
- We propose a GMFlow framework that realizes the global matching formulation for optical flow, which

consists of three main components: a customized Transformer for global feature enhancement, a correlation and softmax layer for feature matching, and a self-attention layer for flow propagation.

- We further propose a refinement step to exploit higher-resolution feature maps, which allows us to reuse the same GMFlow framework to match within local windows for residual flow estimation.
- GMFlow outperforms 32-iteration RAFT’s performance on the challenging Sintel benchmark, while using only one refinement and running faster, offering new possibilities for efficient and accurate optical flow estimation.

2. Related Work

Flow estimation approach. The flow estimation approach is fundamental to existing popular optical flow frameworks, like coarse-to-fine method PWC-Net [35] and iterative method RAFT [38]. They both perform some sort of multi-stage refinements, either at multi-scales [35] or a single resolution [38]. For flow prediction at every single stage, their pipeline is conceptual similar, *i.e.*, regressing optical flow from a local cost volume with convolutions. However, such a flow regression approach has intrinsic limitations, *i.e.*, it is hard to handle large displacements. Thus multi-stage refinements are required to estimate large motion incrementally. The success of RAFT largely lies in the large number of iterative refinements it can perform. Distinct from these approaches, we completely revamp the flow estimation pipeline and show it is indeed possible to achieve highly accurate results while without relying on a large number of refinements.

Large displacements. Large displacements have been a long-standing challenge for optical flow [1–3, 7, 43], in both performance and efficiency. Large motion is usually accompanied with significant appearance change and occlusion, which makes matching corresponding pixels especially challenging. Besides, the massive 2D search space will also introduce too much computational overhead. One popular strategy is to use the coarse-to-fine approach [3, 14, 35] that estimates large motion incrementally. However, coarse-to-fine methods tend to miss fast-moving small objects [31] if the resolution is too coarse. To alleviate this issue, RAFT [38] proposes to maintain a single high-resolution feature and refine the initial prediction with a large number of iterative refinements, achieving state-of-the-art performance on standard benchmarks. However, such a large number of sequential refinements introduce linearly increased inference time, making it hard for speed optimization and hinders its integration into real-time systems. In contrast, our new framework estimates large displacements with both high accuracy and efficiency, achieved by a reformulation of the optical flow problem.

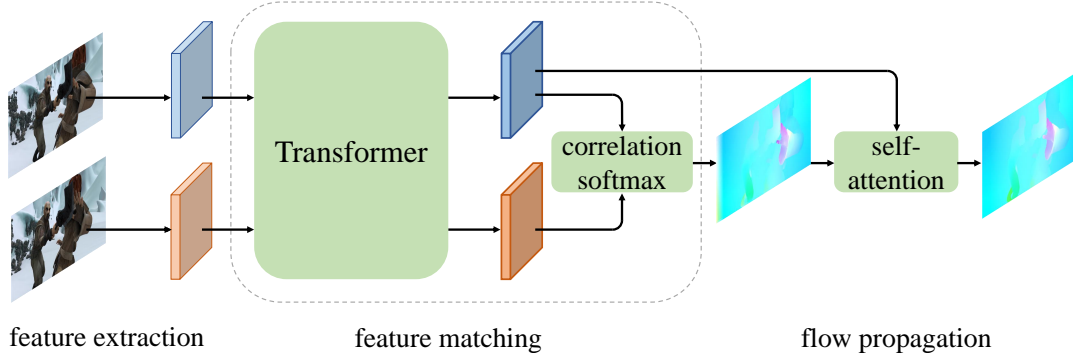


Figure 2. **Overview of our GMFlow framework.** We first extract $8\times$ downsampled features from the input image pair. Then two sets of features are fed to a Transformer that consists of self- and cross-attentions to obtain more discriminative features. The optical flow is later obtained by a differentiable matching layer, which first normalizes the feature correlations with a softmax layer, and then finds the correspondence by taking a weighted average of the matching probability with respect to the 2D pixel coordinates. An additional self-attention layer is used to propagate high-quality flow prediction in matched pixels to unmatched ones by the feature self-similarity.

Transformer for correspondences. SuperGlue [33] pioneered the use of Transformer for sparse feature matching. LoFTR [37] further improves its performance by removing the feature detection step in the typical pipelines. COTR [18] formulates the correspondence problem as a functional mapping by querying the interest point and uses a Transformer as the function. These frameworks are mainly designed for sparse matching problems, and it is non-trivial to directly extend them to dense correspondence tasks. Although COTR in principle can also predict dense correspondences by querying every pixel location, the inference speed is significantly slow. For dense correspondences, STTR [22] is a Transformer-based method for stereo matching, which is a 1D search problem and can be viewed as a special case of optical flow. Importantly, our motivation originates from a deep analysis of existing optical flow methods and a new formulation of optical flow estimation, which is naturally suitable for modelling with Transformers.

3. Methodology

Optical flow is intuitively a matching problem that aims at finding corresponding pixels. To achieve this, we can compare the similarity of the features for each pixel, and identify the corresponding pixel that gives the highest similarity. Such a process requires the features are discriminative enough to stand out. Aggregating the spatial contexts within the image itself and information from another image can intuitively alleviate ambiguities and improve their distinctiveness. Such design philosophies have enabled great achievement in sparse feature matching frameworks [33, 37]. The success of sparse matching, which usually features a large viewpoint change, motivates us to formulate optical flow as an explicit global matching problem in order to address the issue of large displacements.

In the following, we first provide a general description

of our global matching formulation, and then present a Transformer-based framework to realize it.

3.1. Formulation

Given two consecutive video frames I_1 and I_2 , we first extract downsampled dense features $F_1, F_2 \in \mathbb{R}^{H \times W \times D}$ with a shared backbone network, where H, W and D denote height, width and feature dimension, respectively. Considering the corresponding pixels in the two frames should share high similarity, we first compare the feature similarity for each pixel in F_1 with respect to all pixels in F_2 by computing their correlations [41]. This process can be implemented efficiently with a simple matrix multiplication:

$$C = \frac{F_1 F_2^T}{\sqrt{D}} \in \mathbb{R}^{H \times W \times H \times W}, \quad (1)$$

where each element in the correlation matrix C represents the correlation value between coordinates $p_1 = (i, j)$ in F_1 and $p_2 = (k, l)$ in F_2 , and $\frac{1}{\sqrt{D}}$ is a normalization factor to avoid large values after the dot-product operation [39].

To identify the correspondence, one naïve approach is to directly take the location that gives the largest correlation. However, this operation is unfortunately non-differentiable, which prevents end-to-end training. To tackle this issue, we use a differentiable matching layer [19, 41, 45]. Specifically, we normalize the last two dimensions of C with the softmax operation, providing a distribution over the matching probabilities

$$M = \text{softmax}(C) \in \mathbb{R}^{H \times W \times H \times W} \quad (2)$$

between 2D locations in F_1 and F_2 . Then, the correspondence \hat{G} can be obtained by taking a weighted average of the 2D coordinates of pixel grid $G \in \mathbb{R}^{H \times W \times 2}$ with the matching probability M , *i.e.*,

$$\hat{G} = M G \in \mathbb{R}^{H \times W \times 2}. \quad (3)$$

Finally, the optical flow V can be obtained by computing the difference between the corresponding pixel coordinates

$$V = \hat{G} - G \in \mathbb{R}^{H \times W \times 2}. \quad (4)$$

Such a softmax based method can not only enable end-to-end training but also provide sub-pixel accuracy.

3.2. Feature Enhancement

Key to our formulation is to obtain high-quality discriminative features for matching. Recall that the features F_1 and F_2 in Sec. 3.1 are extracted *independently* from a backbone network. To further consider their mutual dependencies, our goal here is to find a function f , such that it can generate more discriminative refined features \hat{F}_1 and \hat{F}_2 , *i.e.*,

$$f : (F_1, F_2) \rightarrow (\hat{F}_1, \hat{F}_2). \quad (5)$$

To achieve this, a natural choice is Transformers [39], which is particularly suitable for modeling the mutual relationship between two sets with the attention mechanism, as demonstrated in sparse matching methods [33, 37]. Since F_1 and F_2 are only two sets of features, they have no notion of the spatial position, we first add the fixed 2D sine and cosine positional encodings (following DETR [6]) to the features. Adding the position information also makes the matching process consider not only the feature similarity but also their spatial distance, which can help resolve ambiguities and improve the performance (see Table 2).

After adding the position information, we perform several stacked self-, cross-attentions and feed-forward network (FFN, *i.e.*, MLP) [39] to improve the representation power of the initial features. Specifically, for self-attention, the query, key and value in the attention computation [39] are the same feature. For cross-attention, the key and value are same but different from the query to introduce their mutual dependencies. This process is performed for both F_1 and F_2 symmetrically, *i.e.*,

$$\hat{F}_1 = \mathcal{T}(F_1 + P, F_2 + P), \quad \hat{F}_2 = \mathcal{T}(F_2 + P, F_1 + P), \quad (6)$$

where \mathcal{T} is a Transformer, P is the positional encoding, the first input of \mathcal{T} is the query and the second input is the key and value. The detailed architectures for the Transformer are given in supplementary material.

One issue in the standard Transformer architecture [39] is the quadratic computational complexity due to the pairwise attention operation. To improve the efficiency, we adopt Swin Transformer [24]’s shifted local window attention strategy. Specifically, we split the input feature of size $H \times W$ to $K \times K$ windows of size $\frac{H}{K} \times \frac{W}{K}$, and perform self- and cross-attentions within each local window independently. For every consecutive local windows, we shift the window partition by $(\frac{H}{2K}, \frac{W}{2K})$ to introduce cross-window connections. In our framework, we split to 2×2 windows of size $\frac{H}{2} \times \frac{W}{2}$, which represents a good speed-accuracy trade-off (see Table 3).

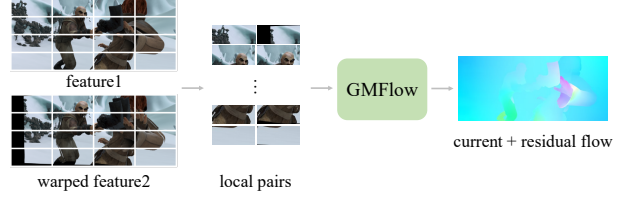


Figure 3. **Our refinement architecture.** The second feature is first warped with the current flow prediction to turn the refinement task to residual flow prediction, which enables the same GMFlow architecture can be used for matching. The only difference is that the matching space is local, which is implemented by splitting the features to non-overlapping windows and performing matching within each window *independently*. The predicted residual flow is added to the current flow prediction as the output.

3.3. Flow Propagation

Our softmax based flow estimation method implicitly assumes that the corresponding pixels are visible in both images and thus can be matched by comparing their similarities. However, this assumption will be invalid for occluded and out-of-boundary pixels (*i.e.*, moving out of the image plane). To remedy this, by observing that the optical flow field and the image itself share high structure similarity [17], we thus propose to propagate the high-quality flow predictions to unmatched pixels by measuring the image/feature self-similarity. This operation can be implemented efficiently with a simple self-attention layer (illustrated in Fig. 2):

$$\tilde{V} = \text{softmax} \left(\frac{\hat{F}_1 \hat{F}_1^T}{\sqrt{D}} \right) \hat{V} \in \mathbb{R}^{H \times W \times 2}, \quad (7)$$

where

$$\hat{V} = \text{softmax} \left(\frac{\hat{F}_1 \hat{F}_2^T}{\sqrt{D}} \right) G - G, \quad (8)$$

is the optical flow from the softmax layer, which is obtained by substituting the refined features in Eq. (5) into the softmax matching layer in Sec. 3.1. Fig. 2 provides an overview of our framework.

3.4. Refinement

The framework presented before (based on 1/8 features) can already achieve competitive performance (see Table 6). It can be further improved by introducing additional higher-resolution (1/4) features for refinement. Specifically, we first upsample the previous 1/8 flow prediction to 1/4 resolution, and warp the second feature with the current flow prediction. Then the refinement task is reduced to the residual flow learning, where the same GMFlow method depicted in Fig. 2 can be used but in a local space. Specifically, considering the 1/4 resolution is too high to perform global attention and the purpose of local refinement, we split the

high-resolution features into 8×8 non-overlapping local windows (each is of $1/32$ of original image resolution) and perform GMFlow within each window *independently*. After obtaining the flow prediction from the softmax layer, we perform a local window (with size 3×3) self-attention operation for flow propagation.

Note that here we share the Transformer and self-attention weights for the global matching and the flow propagation in this refinement stage, which not only reduces parameters but also improves the generalization. To generate the $1/4$ and $1/8$ features, we also share the backbone features. Specifically, we take a similar approach to TridentNet [21] but use a weight-sharing convolution with strides 1 and 2, respectively. Such a weight-sharing design also leads to better performance than the feature pyramid network [23] (see Table 5). Fig. 3 illustrates the refinement architecture. More details are provided in supplementary material.

3.5. Training Loss

We supervise all flow predictions using ℓ_1 loss between the ground truth:

$$L = \sum_{i=1}^N \gamma^{N-i} \|\mathbf{V}_i - \mathbf{V}_{\text{gt}}\|_1, \quad (9)$$

where N is the number of flow predictions including the intermediate and final ones, and γ (set to 0.9) is the weight that is exponentially increasing to give higher weights for later predictions following RAFT [38].

4. Experiments

Datasets and evaluation setup. Following previous methods [16, 35, 38], we first train on the FlyingChairs [10] and FlyingThings3D [27] datasets, then evaluate the cross-dataset generalization ability on Sintel [4] and KITTI [28] training sets. We also evaluate on the FlyingThings3D validation set to see how the model performs on the same domain data. This evaluation setup is used for ablation experiments in Sec. 4.1 and comparisons with RAFT in Sec. 4.2. Next, we perform additional fine-tuning on Sintel and KITTI training sets and report the performance on the online benchmarks in Sec. 4.3.

Metrics. We adopt the commonly used metric in optical flow, *i.e.*, the end-point-error (EPE), which is the average ℓ_2 distance between the prediction and ground truth. For the KITTI’s experiment in addition to EPE, we also report *F1-all*, reflecting the percentage of outliers. To better reflect the performance gains, detailed results, *i.e.*, EPE in different motion magnitudes, are additionally provided. Specifically, we use s_{0-10} , s_{10-40} and s_{40+} , to denote the EPE over pixels with ground truth flow motion magnitude falling to $0 - 10$, $10 - 40$ and more than 40 pixels, respectively.

Implementation details. We implement our full framework in PyTorch 1.9.0. Our backbone network is identical to the RAFT’s model, except that our final feature dimension is 128, while RAFT’s is 256. Both features are at $1/8$ resolution. When generating the $1/4$ and $1/8$ features, we replace the final 2-stride convolution layer in the backbone with stride 1, which produces $1/4$ feature. Then similar to TridentNet [21], we use a weight-sharing convolution with strides 1 and 2 to obtain features at $1/4$ and $1/8$ resolutions, respectively. We stack 6 Transformer blocks for feature matching. To upsample the low-resolution flow prediction to the original image resolution, we use RAFT’s convex upsampling [38] method. We use AdamW [25] as the optimizer. We first train the model on FlyingChairs dataset for 100K iterations, with a batch size of 16 and a learning rate of $4e-4$. We then fine-tune it on FlyingThings3D dataset for 200K iterations, with a batch size of 8 and a learning rate of $2e-4$. For the fine-tuning process on Sintel and KITTI datasets, we report the details in Sec. 4.3. Further details are provided in supplementary material.

4.1. Ablations

Flow estimation approach. We compare our Transformer and softmax based flow estimation method with the cost volume and convolution based approach. Specifically, we adopt the state-of-the-art cost volume construction method in RAFT [38] that concatenates 4 local cost volumes at 4 scales, where each cost volume has a dimension size of $H \times W \times (2R+1)^2$, where H and W are image height and width, respectively, and the search range R is set to 4 following RAFT, which corresponds to a range of 256 pixels at the original image resolution. To regress flow, we stack different number of convolutional residual blocks [12] to see how the performance varies. The final optical flow is obtained from a 3×3 convolution with 2 output channels. For our proposed framework, we stack different number of Transformer blocks for feature enhancement, where one Transformer block consists of self-, cross-attentions and a feed-forward network (FFN). The final optical flow is predicted with a correlation and softmax layer. The results in Table 1 demonstrate that the performance improvement of our method is more significant compared to the cost volume and convolution based approach. For instance, our method with 2 Transformer blocks can already outperform 8 convolution blocks, especially for large motion (s_{40+}). The performance can be further improved by stacking more layers, surpassing the cost volume and convolution based approach by a large margin.

Transformer components. We also provide an ablation study about the different Transformer components in Table 2 to reflect their contributions to the final results. It can be seen that the cross-attention is the most contributing module, thanks to the mutual relationship between two fea-

Method	#blocks	Things (val, clean)				Sintel (train, clean)				Sintel (train, final)				Param (M)
		EPE	s_{0-10}	s_{10-40}	s_{40+}	EPE	s_{0-10}	s_{10-40}	s_{40+}	EPE	s_{0-10}	s_{10-40}	s_{40+}	
cost volume + conv	0	18.83	3.42	6.49	49.65	6.45	1.75	7.17	38.19	7.75	2.10	8.88	45.29	1.8
	4	10.99	1.70	3.41	29.78	3.32	0.73	3.84	20.58	4.93	0.99	5.71	31.16	4.6
	8	9.59	1.44	2.96	26.04	2.89	0.65	3.36	17.75	4.32	0.88	4.95	27.33	8.0
	12	9.04	1.37	2.84	24.46	2.78	0.65	3.32	16.69	4.07	0.84	4.76	25.44	11.5
	18	8.67	1.33	2.74	23.43	2.61	0.59	3.07	15.91	3.94	0.82	4.62	24.58	15.7
Transformer + softmax	0	22.93	8.57	11.13	52.07	8.44	2.71	11.60	42.10	10.28	3.11	13.83	53.34	1.0
	1	11.45	2.98	4.68	28.35	4.12	1.27	5.08	22.25	6.11	1.70	7.89	33.52	1.6
	2	8.59	1.80	3.28	21.99	3.09	0.90	3.66	17.37	4.54	1.24	5.44	26.00	2.1
	4	7.19	1.40	2.62	18.66	2.43	0.67	2.73	14.23	3.78	1.01	4.27	22.37	3.1
	6	6.67	1.26	2.40	17.37	2.28	0.58	2.49	13.89	3.44	0.80	3.97	21.02	4.2

Table 1. **Methodology comparison.** We stack different number of convolutional residual blocks or Transformer blocks (#blocks) to see how the performance varies. All models are trained on FlyingChairs and FlyingThings3D (Things) training sets. We report the performance on FlyingThings3D validation set and the cross-dataset generalization results on Sintel train clean and final sets. The end-point-error (EPE) in different motion magnitude (s_{0-10} , s_{10-40} and s_{40+}) is also reported.

Setup	Things (val)		Sintel (train)		Param (M)
	clean	final	clean	final	
Full	6.67	6.49	2.28	3.44	4.2
w/o cross	10.84	10.61	4.48	6.32	3.8
w/o pos	8.38	8.29	2.85	4.28	4.2
w/o FFN	8.71	8.52	3.1	4.43	1.8
w/o self	7.04	6.88	2.49	3.69	3.8

Table 2. Ablation of different **Transformer components**, *i.e.*, self-attention (self), cross-attention (cross), feed-forward-network (FFN) and positional encoding (pos).

#splits	Things (val, clean)				Time (ms)
	EPE	s_{0-10}	s_{10-40}	s_{40+}	
1×1	6.34	1.26	2.37	16.36	105
2×2	6.67	1.26	2.40	17.37	53
4×4	7.32	1.29	2.58	19.26	35

Table 3. Speed-accuracy trade-off of **different numbers of splits** in shifted local window attention.

tures it encodes. Also, the results benefit from the position information, which makes the matching process position-dependent, and can be conducive to alleviate the ambiguities in pure feature similarity based matching. Removing the feed-forward network (FFN) reduces a large number of parameters, while also leading to a moderate performance drop. The self-attention aggregates contextual cues within the same feature, bringing additional performance gains.

Local window attention. We compare the speed and accuracy of splitting to different numbers of local windows for attention computation in Table 3. Considering the extracted features from the backbone is of $1/8$ resolution, further splitting to $H/2 \times W/2$ local windows (*i.e.*, $1/16$ of

prop.	Sintel (clean)			Sintel (final)		
	all	matched	unmatched	all	matched	unmatched
w/o	2.28	1.06	15.54	3.44	1.95	19.50
w/	1.89	1.10	10.39	3.13	1.98	15.52

Table 4. Effectiveness of **flow propagation (prop.) with self-attention.**

Setup	Share Trans?	Share Feature?	Things	Sintel (train)		Param (M)
			clean	clean	final	
w/o refine	-	-	4.10	1.64	3.04	4.7
w/ refine	✓	✓	3.90	1.38	2.98	8.0
			3.78	1.31	2.93	4.9
	✓	✓	3.64	1.31	2.66	4.7

Table 5. Effectiveness of **sharing Transformer and multi-scale features** in the refinement architecture.

the original resolution) represents a good trade-off between accuracy and speed, and thus is used in our framework.

Flow propagation. Our flow propagation strategy results in significant performance gains in unmatched regions (including occlusion and out-of-boundary pixels), as demonstrated in Table 4. The structural correlation between the image and flow provides a strong clue to improve the performance of pixels that are challenging to match.

Refinement. There are two design choices in the refinement architecture: whether to share the convolution backbone to extract $1/8$ and $1/4$ features, and whether to share the Transformer for matching at $1/8$ and $1/4$ resolution. The comparison results are shown in Table 5. Sharing Transformer and multi-scale features better regularizes the

Method	#iter	Things (val, clean)				Sintel (train, clean)				Sintel (train, final)				Param (M)	Time (ms)
		EPE	s_{0-10}	s_{10-40}	s_{40+}	EPE	s_{0-10}	s_{10-40}	s_{40+}	EPE	s_{0-10}	s_{10-40}	s_{40+}		
RAFT [38]	1	14.28	1.47	3.62	40.48	4.04	0.77	4.30	26.66	5.45	0.99	6.30	35.19	5.3	25 (14)
	4	6.27	0.69	1.67	17.63	1.92	0.47	2.32	11.37	3.25	0.65	4.00	20.04		39 (21)
	8	4.66	0.55	1.38	12.87	1.61	0.39	1.90	9.61	2.80	0.53	3.30	17.76		58 (31)
	12	4.31	0.53	1.33	11.79	1.55	0.41	1.73	9.19	2.72	0.52	3.12	17.43		78 (41)
	24	4.22	0.53	1.32	11.52	1.47	0.36	1.63	9.00	2.69	0.52	3.05	17.28		133 (71)
	32	4.25	0.53	1.31	11.63	1.41	0.32	1.55	8.83	2.69	0.52	3.00	17.45		170 (91)
GMFlow	1	4.10	0.74	1.59	10.55	1.64	0.48	1.99	9.11	3.04	0.76	3.74	17.71	4.7	57 (26)
	2	3.64	0.70	1.36	9.40	1.31	0.34	1.51	7.79	2.66	0.59	3.15	16.31	4.7	126 (57)

Table 6. **RAFT’s iterative framework vs. our GMFlow framework.** The models are trained on FlyingChairs and FlyingThings3D training sets. We use RAFT’s officially released model for evaluation. We denote our model without refinement as 1 iteration, and with refinement as 2 iterations. The inference time is measured on a single V100 and A100 (in parentheses) GPU at Sintel resolution (436×1024). Our framework gains more speedup than RAFT ($2.21\times$ vs. $1.87\times$, *i.e.*, ours: $126 \rightarrow 57$, RAFT: $170 \rightarrow 91$) on the high-end A100 GPU since our method doesn’t require a large number of sequential computation.

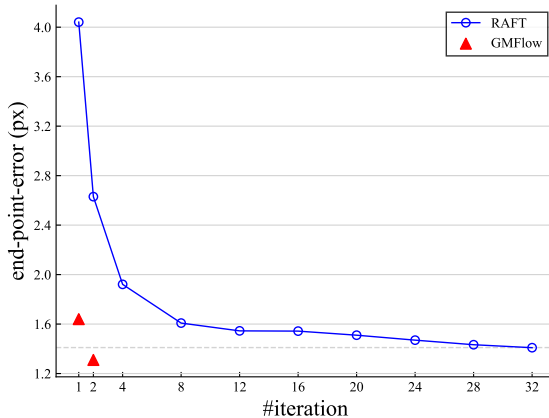


Figure 4. Optical flow **end-point-error vs. number of iterations** at inference time. This figure shows the generalization results on Sintel (clean) training set after training on FlyingChairs and FlyingThings3D datasets. Our method outperforms 32-iteration RAFT’s performance, while using only one refinement (denoted as 2 iterations) and running faster. See Table 6 for details.

Training data	Method	EPE	F1-all	s_{0-10}	s_{10-40}	s_{40+}
C + T	RAFT	5.35	17.46	0.67	1.57	13.79
	GMFlow	11.45	29.27	0.78	2.62	30.90
C + T + VK	RAFT	2.77	8.30	0.53	1.41	6.30
	GMFlow	3.21	11.47	0.57	1.32	7.69

Table 7. Generalization on KITTI after training on synthetic datasets FlyingChairs (C), FlyingThings3D (T) and Virtual KITTI 2 (VK).

learning process towards a universal matching function and feature representations, leading to a better in-domain performance and generalization, especially on the challenging Sintel (final) dataset.

4.2. Comparison with RAFT

Results on Sintel. Table 6 shows the results on FlyingThings3D validation set and Sintel clean and final training set after training on FlyingChairs and FlyingThings3D training sets. Without using any iterations, our method achieves comparable performance with RAFT after 8 iterations. By using an additional refinement, our method outperforms RAFT after 32 iterations, especially on the large motion (s_{40+}). Fig. 4 visualizes the results. Furthermore, our framework enjoys a faster inference speed compared to the state-of-the-art method RAFT and also does not require a large number of sequential processing. On the high-end A100 GPU, our framework gains more speedup compared with RAFT’s sequential framework ($2.21\times$ vs. $1.87\times$, *i.e.*, ours: $126 \rightarrow 57$, RAFT: $170 \rightarrow 91$), reflecting our framework can benefit more from advanced hardware acceleration and showing its potential for further speed optimization and integration into real-world applications.

Results on KITTI. Table 7 shows the generalization results on KITTI training set after training on FlyingChairs and FlyingThings3D datasets. In this evaluation setting, our framework doesn’t outperform RAFT, which is mainly caused by the large domain gap between the synthetic training sets and the real-world evaluation dataset. The main reason behind our inferior performance in this setting is that RAFT, relying on fully convolutional neural networks, benefits from the inductive biases in convolution layers, which requires a relatively smaller size training data to generalize to a new dataset in comparison with Transformers [8, 9, 46]. To substantiate this claim, we also fine-tune both RAFT and our method on the additional Virtual KITTI 2 [5] dataset. We can see from Table 7 that the performance gap becomes smaller when more data is available for training.

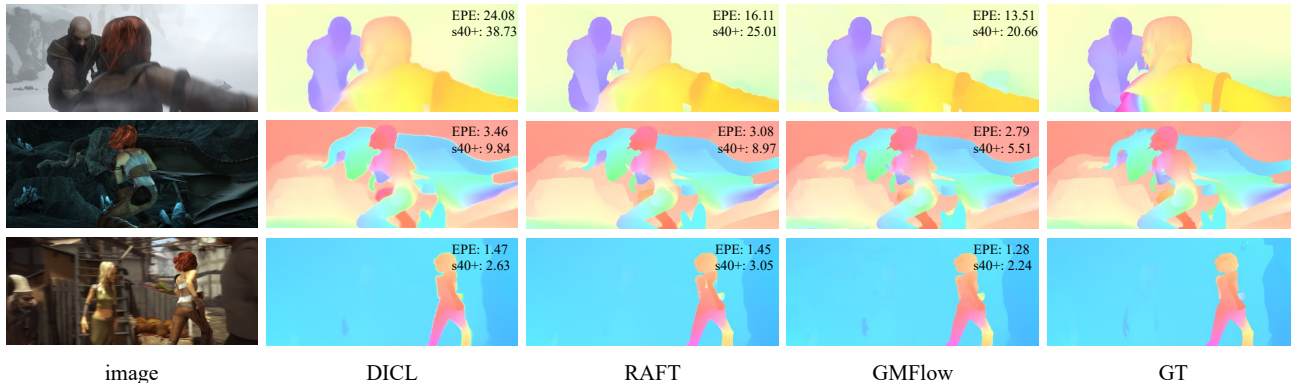


Figure 5. Visual comparisons on Sintel test set.

Method	Sintel (clean)			Sintel (final)		
	all	matched	unmatched	all	matched	unmatched
FlowNet2 [16]	4.16	1.56	25.40	5.74	2.75	30.11
PWC-Net+ [36]	3.45	1.41	20.12	4.60	2.25	23.70
HD ³ [48]	4.79	1.62	30.63	4.67	2.17	24.99
VCN [47]	2.81	1.11	16.68	4.40	2.22	22.24
DICL [40]	2.63	0.97	16.24	3.60	1.66	19.44
RAFT [38]	1.94	-	-	3.18	-	-
GMFlow	1.87	0.69	11.47	3.11	1.38	17.16
RAFT [†] [38]	1.61	0.62	9.65	2.86	1.41	14.68

Table 8. Comparison results on Sintel test set. [†] represents the method uses previous frame’s prediction as initialization for subsequent refinement, while other methods all use two frames only.

4.3. Comparison on Benchmarks

Sintel. Following previous works [38, 44], we fine-tune our pre-trained model on a mixed dataset that consists of KITTI [28], HD1K [20], FlyingThings3D [27] and Sintel [4] training sets. We perform our model’s fine-tuning for 200K iterations with a batch size of 8 and a learning rate of $2e-4$. The results on Sintel test set are shown in Table 8. We achieve the best performance among all the competitive state-of-the-art methods that only use two frames during prediction. Note that RAFT’s performance can be improved by using previous frame’s prediction as initialization for subsequent refinement. However, we note that we still achieve comparable performance with RAFT in matched regions even without using multi-frame information. Qualitative comparisons between our GMFlow and the other state-of-the-art approaches on Sintel test set are shown in Fig. 5.

KITTI. We perform additional fine-tuning on the KITTI 2015 training set from our model pre-trained on Sintel. We train GMFlow for 100K iterations with a batch size of 8 and a learning rate of $2e-4$. Table 9 shows the evaluation results. For non-occluded (Noc) pixels, our performance is slightly inferior to RAFT. For all pixels that contain both non-occluded and occluded pixels, the performance gap becomes larger. Our inferior performance is mainly due to the very limited training data available in KITTI.

Method	FlowNet2 [16]	PWC-Net+ [36]	RAFT [38]	GMFlow
All	11.48	7.72	5.10	9.71
Noc	6.94	4.91	3.07	4.28

Table 9. Comparisons on KITTI test set, the metric is F1-all. “All” denotes the evaluation results on all pixels with ground truth, and “Noc” denotes non-occluded pixels only.

4.4. Limitation and Discussion

Our framework may not generalize well when the size of the training data is small and/or the training data has significantly large domain gap with the test data (*e.g.*, synthetic FlyingThings3D to real-world KITTI). This is mainly due to the Transformer based design. Unlike convolutional networks, Transformer models do not carry important inductive biases and therefore require training on large scale datasets to generalize well on the unseen domains [8, 9, 46]. Fortunately, there are many large scale datasets available currently, *e.g.*, Virtual KITTI [5, 11], VIPER [32], RE-FRESH [26], AutoFlow [34] and TartanAir [42], they can be used to enhance Transformers’ generalization ability.

5. Conclusion

We have presented a new framework for efficient and accurate optical flow estimation. Key to our approach is a reformulation of optical flow as an explicit matching problem between two sets of deep features. Such a new perspective naturally enables us to model the matching process globally using a Transformer. We outperform 32-iteration RAFT’s performance on the challenging Sintel dataset, while only using one refinement and running faster. We hope our new perspective will pave a way towards a new paradigm for efficient and accurate optical flow estimation.

Broader impact. Our proposed method might produce unreliable results in challenging cases like occlusions, thus care should be taken when using the prediction results from our model, especially for safety-critical scenarios like self-driving cars. This issue also calls for future research to take the robustness of the proposed method into consideration.

References

- [1] Christian Bailer, Bertram Taetz, and Didier Stricker. Flow fields: Dense correspondence fields for highly accurate large displacement optical flow estimation. In *Proceedings of the IEEE International Conference on Computer Vision*, pages 4015–4023, 2015. 2
- [2] Thomas Brox, Christoph Bregler, and Jitendra Malik. Large displacement optical flow. In *Proceedings of the IEEE International Conference on Computer Vision*, pages 41–48. IEEE, 2009. 2
- [3] Thomas Brox, Andrés Bruhn, Nils Papenberg, and Joachim Weickert. High accuracy optical flow estimation based on a theory for warping. In *European Conference on Computer Vision*, pages 25–36. Springer, 2004. 2
- [4] Daniel J Butler, Jonas Wulff, Garrett B Stanley, and Michael J Black. A naturalistic open source movie for optical flow evaluation. In *European Conference on Computer Vision*, pages 611–625. Springer, 2012. 5, 8
- [5] Yohann Cabon, Naila Murray, and Martin Humenberger. Virtual kitti 2. *arXiv preprint arXiv:2001.10773*, 2020. 7, 8
- [6] Nicolas Carion, Francisco Massa, Gabriel Synnaeve, Nicolas Usunier, Alexander Kirillov, and Sergey Zagoruyko. End-to-end object detection with transformers. In *European Conference on Computer Vision*, pages 213–229. Springer, 2020. 4
- [7] Zhuoyuan Chen, Hailin Jin, Zhe Lin, Scott Cohen, and Ying Wu. Large displacement optical flow from nearest neighbor fields. In *Proceedings of the IEEE Conference on Computer Vision and Pattern Recognition*, pages 2443–2450, 2013. 2
- [8] Stéphane d’Ascoli, Hugo Touvron, Matthew Leavitt, Ari Morcos, Giulio Biroli, and Levent Sagun. Convit: Improving vision transformers with soft convolutional inductive biases. *International Conference on Machine Learning*, 2021. 7, 8
- [9] Alexey Dosovitskiy, Lucas Beyer, Alexander Kolesnikov, Dirk Weissenborn, Xiaohua Zhai, Thomas Unterthiner, Mostafa Dehghani, Matthias Minderer, Georg Heigold, Sylvain Gelly, Jakob Uszkoreit, and Neil Houlsby. An image is worth 16x16 words: Transformers for image recognition at scale. *International Conference on Learning Representations*, 2021. 7, 8
- [10] Alexey Dosovitskiy, Philipp Fischer, Eddy Ilg, Philip Hausser, Caner Hazirbas, Vladimir Golkov, Patrick Van Der Smagt, Daniel Cremers, and Thomas Brox. FlowNet: Learning optical flow with convolutional networks. In *Proceedings of the IEEE International Conference on Computer Vision*, pages 2758–2766, 2015. 1, 5
- [11] Adrien Gaidon, Qiao Wang, Yohann Cabon, and Eleonora Vig. Virtual worlds as proxy for multi-object tracking analysis. In *Proceedings of the IEEE Conference on Computer Vision and Pattern Recognition*, pages 4340–4349, 2016. 8
- [12] Kaiming He, Xiangyu Zhang, Shaoqing Ren, and Jian Sun. Deep residual learning for image recognition. In *Proceedings of the IEEE Conference on Computer Vision and Pattern Recognition*, pages 770–778, 2016. 5
- [13] Asmaa Hosni, Christoph Rhemann, Michael Bleyer, Carsten Rother, and Margrit Gelautz. Fast cost-volume filtering for visual correspondence and beyond. *IEEE Transactions on Pattern Analysis and Machine Intelligence*, 35(2):504–511, 2012. 1
- [14] Yinlin Hu, Rui Song, and Yunsong Li. Efficient coarse-to-fine patchmatch for large displacement optical flow. In *Proceedings of the IEEE Conference on Computer Vision and Pattern Recognition*, pages 5704–5712, 2016. 2
- [15] Junhwa Hur and Stefan Roth. Iterative residual refinement for joint optical flow and occlusion estimation. In *Proceedings of the IEEE/CVF Conference on Computer Vision and Pattern Recognition*, pages 5754–5763, 2019. 1
- [16] Eddy Ilg, Nikolaus Mayer, Tonmoy Saikia, Margret Keuper, Alexey Dosovitskiy, and Thomas Brox. FlowNet 2.0: Evolution of optical flow estimation with deep networks. In *Proceedings of the IEEE Conference on Computer Vision and Pattern Recognition*, pages 2462–2470, 2017. 1, 5, 8
- [17] Shihao Jiang, Dylan Campbell, Yao Lu, Hongdong Li, and Richard Hartley. Learning to estimate hidden motions with global motion aggregation. In *Proceedings of the IEEE/CVF International Conference on Computer Vision*, pages 9772–9781, October 2021. 1, 4
- [18] Wei Jiang, Eduard Trulls, Jan Hosang, Andrea Tagliasacchi, and Kwang Moo Yi. Cotr: Correspondence transformer for matching across images. *Proceedings of the IEEE/CVF International Conference on Computer Vision*, 2021. 3
- [19] Alex Kendall, Hayk Martirosyan, Saumitro Dasgupta, Peter Henry, Ryan Kennedy, Abraham Bachrach, and Adam Bry. End-to-end learning of geometry and context for deep stereo regression. In *Proceedings of the IEEE International Conference on Computer Vision*, pages 66–75, 2017. 3
- [20] Daniel Kondermann, Rahul Nair, Katrin Honauer, Karsten Krispin, Jonas Andrulis, Alexander Brock, Burkhard Gussefeld, Mohsen Rahimimoghaddam, Sabine Hofmann, Claus Brenner, et al. The hci benchmark suite: Stereo and flow ground truth with uncertainties for urban autonomous driving. In *Proceedings of the IEEE Conference on Computer Vision and Pattern Recognition Workshops*, pages 19–28, 2016. 8
- [21] Yanghao Li, Yuntao Chen, Naiyan Wang, and Zhaoxiang Zhang. Scale-aware trident networks for object detection. In *Proceedings of the IEEE/CVF International Conference on Computer Vision*, pages 6054–6063, 2019. 5
- [22] Zhaoshuo Li, Xingtong Liu, Nathan Drenkow, Andy Ding, Francis X Creighton, Russell H Taylor, and Mathias Unberath. Revisiting stereo depth estimation from a sequence-to-sequence perspective with transformers. In *Proceedings of the IEEE/CVF International Conference on Computer Vision*, pages 6197–6206, 2021. 3
- [23] Tsung-Yi Lin, Piotr Dollár, Ross Girshick, Kaiming He, Bharath Hariharan, and Serge Belongie. Feature pyramid networks for object detection. In *Proceedings of the IEEE Conference on Computer Vision and Pattern Recognition*, pages 2117–2125, 2017. 5
- [24] Ze Liu, Yutong Lin, Yue Cao, Han Hu, Yixuan Wei, Zheng Zhang, Stephen Lin, and Baining Guo. Swin transformer: Hierarchical vision transformer using shifted windows. *Proceedings of the IEEE/CVF International Conference on Computer Vision*, 2021. 4, 11

- [25] Ilya Loshchilov and Frank Hutter. Decoupled weight decay regularization. *arXiv preprint arXiv:1711.05101*, 2017. 5
- [26] Zhaoyang Lv, Kihwan Kim, Alejandro Troccoli, Deqing Sun, James M Rehg, and Jan Kautz. Learning rigidity in dynamic scenes with a moving camera for 3d motion field estimation. In *European Conference on Computer Vision*, pages 468–484, 2018. 8
- [27] Nikolaus Mayer, Eddy Ilg, Philip Hausser, Philipp Fischer, Daniel Cremers, Alexey Dosovitskiy, and Thomas Brox. A large dataset to train convolutional networks for disparity, optical flow, and scene flow estimation. In *Proceedings of the IEEE Conference on Computer Vision and Pattern Recognition*, pages 4040–4048, 2016. 5, 8
- [28] Moritz Menze and Andreas Geiger. Object scene flow for autonomous vehicles. In *Proceedings of the IEEE Conference on Computer Vision and Pattern Recognition*, pages 3061–3070, 2015. 5, 8
- [29] Federico Perazzi, Jordi Pont-Tuset, Brian McWilliams, Luc Van Gool, Markus Gross, and Alexander Sorkine-Hornung. A benchmark dataset and evaluation methodology for video object segmentation. In *Proceedings of the IEEE Conference on Computer Vision and Pattern Recognition*, pages 724–732, 2016. 11
- [30] Anurag Ranjan and Michael J Black. Optical flow estimation using a spatial pyramid network. In *Proceedings of the IEEE Conference on Computer Vision and Pattern Recognition*, pages 4161–4170, 2017. 1
- [31] Jerome Revaud, Philippe Weinzaepfel, Zaid Harchaoui, and Cordelia Schmid. Epicflow: Edge-preserving interpolation of correspondences for optical flow. In *Proceedings of the IEEE Conference on Computer Vision and Pattern Recognition*, pages 1164–1172, 2015. 2
- [32] Stephan R Richter, Zeeshan Hayder, and Vladlen Koltun. Playing for benchmarks. In *Proceedings of the IEEE International Conference on Computer Vision*, pages 2213–2222, 2017. 8
- [33] Paul-Edouard Sarlin, Daniel DeTone, Tomasz Malisiewicz, and Andrew Rabinovich. Superglue: Learning feature matching with graph neural networks. In *Proceedings of the IEEE/CVF Conference on Computer Vision and Pattern Recognition*, pages 4938–4947, 2020. 1, 2, 3, 4
- [34] Deqing Sun, Daniel Vlasic, Charles Herrmann, Varun Jampani, Michael Krainin, Huiwen Chang, Ramin Zabih, William T Freeman, and Ce Liu. Autoflow: Learning a better training set for optical flow. In *Proceedings of the IEEE/CVF Conference on Computer Vision and Pattern Recognition*, pages 10093–10102, 2021. 8
- [35] Deqing Sun, Xiaodong Yang, Ming-Yu Liu, and Jan Kautz. Pwc-net: Cnns for optical flow using pyramid, warping, and cost volume. In *Proceedings of the IEEE Conference on Computer Vision and Pattern Recognition*, pages 8934–8943, 2018. 1, 2, 5
- [36] Deqing Sun, Xiaodong Yang, Ming-Yu Liu, and Jan Kautz. Models matter, so does training: An empirical study of cnns for optical flow estimation. *IEEE Transactions on Pattern Analysis and Machine Intelligence*, 42(6):1408–1423, 2019. 8
- [37] Jiaming Sun, Zehong Shen, Yuang Wang, Hujun Bao, and Xiaowei Zhou. Loftr: Detector-free local feature matching with transformers. In *Proceedings of the IEEE/CVF Conference on Computer Vision and Pattern Recognition*, pages 8922–8931, 2021. 1, 2, 3, 4
- [38] Zachary Teed and Jia Deng. Raft: Recurrent all-pairs field transforms for optical flow. In *European Conference on Computer Vision*, pages 402–419. Springer, 2020. 1, 2, 5, 7, 8, 11
- [39] Ashish Vaswani, Noam Shazeer, Niki Parmar, Jakob Uszkoreit, Llion Jones, Aidan N Gomez, Łukasz Kaiser, and Illia Polosukhin. Attention is all you need. In *Advances in Neural Information Processing Systems*, pages 5998–6008, 2017. 1, 2, 3, 4
- [40] Jianyuan Wang, Yiran Zhong, Yuchao Dai, Kaihao Zhang, Pan Ji, and Hongdong Li. Displacement-invariant matching cost learning for accurate optical flow estimation. *Advances in Neural Information Processing Systems*, 33, 2020. 8
- [41] Qianqian Wang, Xiaowei Zhou, Bharath Hariharan, and Noah Snavely. Learning feature descriptors using camera pose supervision. In *European Conference on Computer Vision*, pages 757–774. Springer, 2020. 1, 3
- [42] Wenshan Wang, DeLong Zhu, Xiangwei Wang, Yaoyu Hu, Yuheng Qiu, Chen Wang, Yafei Hu, Ashish Kapoor, and Sebastian Scherer. Tartanair: A dataset to push the limits of visual slam. 2020. 8
- [43] Philippe Weinzaepfel, Jerome Revaud, Zaid Harchaoui, and Cordelia Schmid. Deepflow: Large displacement optical flow with deep matching. In *Proceedings of the IEEE International Conference on Computer Vision*, pages 1385–1392, 2013. 2
- [44] Haofei Xu, Jiaolong Yang, Jianfei Cai, Juyong Zhang, and Xin Tong. High-resolution optical flow from 1d attention and correlation. In *Proceedings of the IEEE/CVF International Conference on Computer Vision*, pages 10498–10507, 2021. 1, 8
- [45] Haofei Xu and Juyong Zhang. Aanet: Adaptive aggregation network for efficient stereo matching. In *Proceedings of the IEEE/CVF Conference on Computer Vision and Pattern Recognition*, pages 1959–1968, 2020. 3
- [46] Yufei Xu, Qiming Zhang, Jing Zhang, and Dacheng Tao. Vitae: Vision transformer advanced by exploring intrinsic inductive bias. *Advances in Neural Information Processing Systems*, 2021. 7, 8
- [47] Gengshan Yang and Deva Ramanan. Volumetric correspondence networks for optical flow. *Advances in Neural Information Processing Systems*, 32:794–805, 2019. 8
- [48] Zhichao Yin, Trevor Darrell, and Fisher Yu. Hierarchical discrete distribution decomposition for match density estimation. In *Proceedings of the IEEE Conference on Computer Vision and Pattern Recognition*, pages 6044–6053, 2019. 8
- [49] Feihu Zhang, Oliver J. Woodford, Victor Adrian Prisacariu, and Philip H.S. Torr. Separable flow: Learning motion cost volumes for optical flow estimation. In *Proceedings of the IEEE/CVF International Conference on Computer Vision*, pages 10807–10817, October 2021. 1

Appendix

A. More Comparisons

We present more comprehensive comparisons (as a supplement of Table 1 in the main paper) on all the possible combinations of flow estimation approaches in Table 10. Our Transformer and softmax-based method is consistently more effective and has less parameters than other variants.

B. Computational Complexity

We analyze the computational complexities of core components in our framework below.

Global Matching. In our global matching formulation, we build a 4D correlation matrix $H \times W \times H \times W$ to model all pair-wise similarities between two features (with size $H \times W$, 1/8 of the original image resolution). There exists an equivalent implementation should it become a bottleneck for high-resolution images. Note that the pixels in the first feature are *independent* and thus their flow predictions can be computed *sequentially*. Specifically, we can sequentially compute $K \times K$ correlation matrices (each with size $H/K \times W/K \times H \times W$), and finally merge the results for all pixels. Such a sequential implementation can save the memory consumption while having little influence on the overall inference time (see Table 11), since the global matching operation only needs to compute once, and it’s not a significant speed bottleneck in the full framework.

#splits	1 × 1	2 × 2	4 × 4	8 × 8
Time (ms)	52.57	52.64	52.90	59.45

Table 11. **Inference time vs. different number of splits for sequential global matching implementation.** The input image resolution is 448×1024 , and the features are downsampled by $8 \times$.

We note that our alternative sequential implementation is not possible for previous cost volume and convolution-based approaches (e.g., RAFT [38]), since the cost volume is used as an intermediate component for subsequent regression with convolutions, where all pixels in the spatial dimension are tightly coupled.

Transformer. We use shifted local window attention [24] in the Transformer implementation, where each local window size is 1/16 of the original image resolution. The computational cost is usually acceptable for regular image resolutions (e.g., 448×1024). Note that we can always switch to smaller windows splitting (e.g., 1/32, see Table 3 of the main paper) should it become a bottleneck.

Flow Propagation. Our default flow propagation scheme computes a global self-attention. It’s also possible to compute a local window self-attention only for less memory consumption by trading some accuracy in large motion

(see Table 12). Such a local attention operation can be implemented efficiently with PyTorch’s `unfold` function.

self-attn.	Sintel (train, final)			
	EPE	s_{0-10}	s_{10-40}	s_{40+}
global	3.13	0.80	3.87	18.04
local 3×3	3.31	0.79	3.75	20.22
local 5×5	3.21	0.75	3.66	19.69

Table 12. **Global vs. local self-attention for flow propagation.**

For our refinement architecture, although the feature resolution is higher (1/4), it is not a significant bottleneck since we perform matching within each local window (1/32) independently. Also, shifted local window attention is used in the Transformer implementation (thus 1/64 of the original image resolution).

Overall, our GMFlow framework is general and flexible, and many concrete implementations are possible to meet specific needs.

C. More Visual Results

Flow Propagation. Our flow propagation scheme with self-attention is quite effective for handling occluded and out-of-boundary pixels, as can be seen from Fig. 6.

Prediction on DAVIS dataset. We test our pre-trained Sintel model on the DAVIS [29] dataset, the results on diverse scenes are shown in Fig. 7.

D. More Implementation Details

Network Architectures. The Transformer model in our framework consists of 6 Transformer blocks, where each block consists of a self-attention, cross-attention and feed-forward network (FFN). The Transformer dimension is 128, and the intermediate FFN layer expands the dimension by $4 \times$. We only use a single head in all the attention computations, since we observe multi-head attention slows down the speed while not bringing obvious improvement in performance. Our refinement architecture uses exactly the same Transformer for feature enhancement, except it is performed within each local window independently. The self-attention layer in the flow propagation step is also shared, except that we perform global attention at 1/8 resolution, while local window attention is used at 1/4 resolution.

Training Details. Our data augmentation strategy mostly follows RAFT [38] except that we didn’t use occlusion augmentation, since no obvious improvement is observed in our experiments. During training, we perform random cropping following previous works. The crop size for FlyingChairs is 384×512 , FlyingThings3D is 384×768 , Sintel is 320×896 and KITTI is 320×960 . Our framework without refinement is trained on 4 V100 (16GB) GPUs.

Method	feature enhancement	flow estimation	#convs	Sintel (train, clean)			Sintel (train, final)			Param (M)
				all	matched	unmatched	all	matched	unmatched	
variants	-	cost + conv	14	3.32	1.56	22.34	4.93	2.82	27.73	4.64
	Transformer	cost + conv	2	3.41	2.40	14.32	4.57	3.27	18.67	4.95
	Transformer	cost + conv	14	2.04	1.09	12.34	3.37	2.03	17.80	7.79
	conv	softmax	14	6.36	3.22	40.30	8.00	4.80	42.58	5.12
ours w/o prop.	Transformer	softmax	0	2.28	1.06	15.54	3.44	1.95	19.50	4.20
ours w/ prop.	Transformer	softmax	0	1.89	1.10	10.39	3.13	1.98	15.52	4.23

Table 10. **Comparisons on different variants of flow estimation approaches.** While the Transformer can also be used for feature enhancement in the cost volume and convolution-based approach (cost + conv), its performance heavily relies on a deep convolutional regressor (*e.g.*, 14 layers to catch up). In contrast, our softmax-based method is *parameter-free* (4.20M *vs.* 7.79M). The flow propagation (prop.) layer further improves ours performance in unmatched regions, while only introducing additional 0.03M parameters. Replacing the Transformer with convolutions for feature enhancement leads to significantly large performance drop, since convolutions are not able to model the mutual relationship between two features.

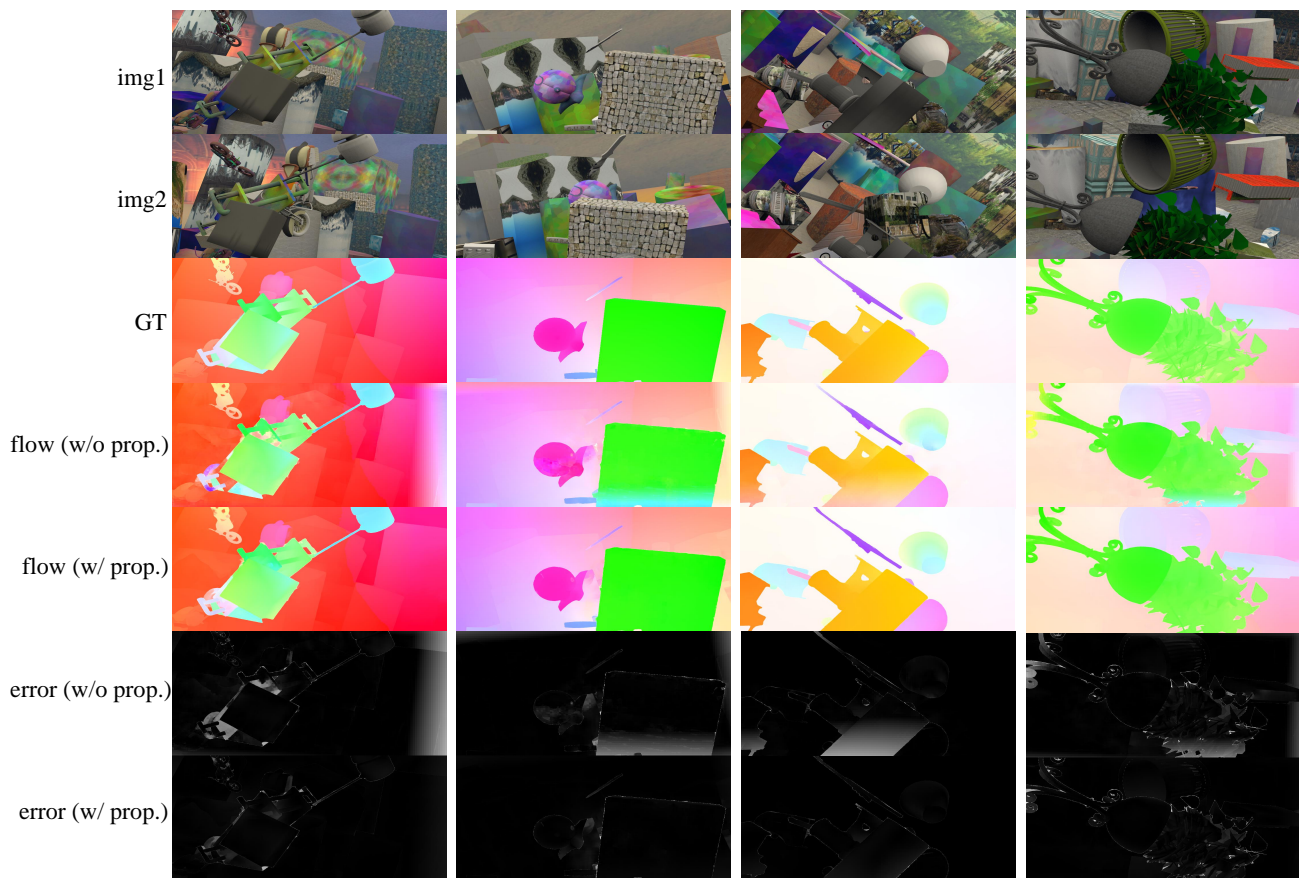


Figure 6. Our flow propagation (prop.) scheme significantly improves the performance of occluded and out-of-boundary pixels.

The full framework with refinement is trained on 4 A100 (40GB) GPUs. We are also able to reproduce the results on 4 V100 (16GB) GPUs by halving the batch size and doubling the training iterations.



Figure 7. Visual results on DAVIS dataset.